



HAL
open science

Validation of a Physically Enhanced Sub Idle Compressor Map Extrapolation Method

Linyuan Jia, Yuchun Chen

► **To cite this version:**

Linyuan Jia, Yuchun Chen. Validation of a Physically Enhanced Sub Idle Compressor Map Extrapolation Method. 16th International Symposium on Transport Phenomena and Dynamics of Rotating Machinery, Apr 2016, Honolulu, United States. hal-01890081

HAL Id: hal-01890081

<https://hal.science/hal-01890081>

Submitted on 8 Oct 2018

HAL is a multi-disciplinary open access archive for the deposit and dissemination of scientific research documents, whether they are published or not. The documents may come from teaching and research institutions in France or abroad, or from public or private research centers.

L'archive ouverte pluridisciplinaire **HAL**, est destinée au dépôt et à la diffusion de documents scientifiques de niveau recherche, publiés ou non, émanant des établissements d'enseignement et de recherche français ou étrangers, des laboratoires publics ou privés.

Validation of a Physically Enhanced Sub Idle Compressor Map Extrapolation Method

Linyuan Jia^{1,2*}, Yuchun Chen¹



Abstract

The objective of this study is to validate the physically enhanced compressor map extrapolation (PECME) method brought forward by Zachos. The essential steps for this method are introduced and carried out in conjunction with the compressor zero speed curve to extrapolate the Allison 250 engine compressor map to the sub idle region. The power extrapolation engine sub idle performance simulation model and the evaporation controlled combustion efficiency model are used in the engine sub idle performance simulation model. The complete compressor map is then used in the engine performance simulation model and the engine starting performance is simulated and validated with the test data. The deviations of the rotational speeds are analyzed, showing that the PECME method is practical and valid. A case study is also carried out by simulating the Allison 250 engine operating process from engine starting to 200Nm load. The simulation results are well matched with the test data which proves that the whole methodology introduced in this paper is able to provide high fidelity simulation results in a wide range of engine operation.

Keywords

Turboshaft engine — compressor map extrapolation — performance simulation — test data correction

¹ School of power and energy, Northwestern Polytechnical University, Xi'an, P.R. China

² Institute for flight propulsion, Technical University of Munich, Munich, Germany

*Corresponding author: jlynpu@live.com

INTRODUCTION

Gas turbine engine starting performance simulation is an inevitable section for engine performance analysis and starting control schedule design. The component maps based model is regarded as the most practical gas turbine engine starting performance simulation model due to the detailed information it provides. However, component maps for sub idle region are usually unavailable. Therefore, several map extrapolation methods were developed.

In 2000, Kurzke developed a tool named Smooth C for compressor map extrapolation based on the estimated zero speed line and some principles deduced from incompressible similarity laws [1, 2]. A different method was developed by Sexton in 2001, in which the exponents of incompressible similarity laws were modified in order to take the compressible effects into consideration [3]. In 2007, Sexton's method was simplified by Gaudet [4, 5], which was then validated by Hönle in 2013 [6]. In 2002, Jones compared the existing map extrapolation methods and suggested that the zero speed line be either calculated, measured or estimated to transform extrapolation into interpolation and to obtain more reliable results [7]. Following Jones' suggestion, in 2007, Howard determined the zero speed curve using the generic coefficients obtained from 3D CFD simulation [8]. The curve was used to generate the compressor sub idle maps. In 2010, Zachos improved Howard's work by employing the locked rotor corrected torque characteristics, thus converting the mathematical map extrapolation method into a physically enhanced interpolation

method with the ability to obtain a more accurate sub idle compressor map [9, 10]. Some remarkable engine performance simulation results were provided by Zachos to show the capability of the PECME method [9]. However, the map extrapolation results along with the engine simulation results are not validated due to the insufficient data available for sub-idle operation.

In 2013, the Allison 250 engine compressor locked rotor characteristics, in forms of pressure ratio and torque curves, were measured by Hönle [6], which makes it possible to extrapolate the compressor map to sub idle region, by employing the PECME method. Therefore, this method can then be validated with test data.

In this paper, the sub idle compressor map of the Allison 250 engine was generated based on locked rotor characteristic measurement data provided by Hönle [6]. The completed compressor map was then used to simulate the starting performance of the Allison 250 engine. Simulation results were then validated with engine starting test data. Some special concerns regarding the validation method, such as the engine sub idle performance modelling and test data correction method are also discussed in this paper.

1. MAP EXTRAPOLATION

The PECME method was developed described in detail in reference [9]. During this section, the essential steps of this method are introduced.

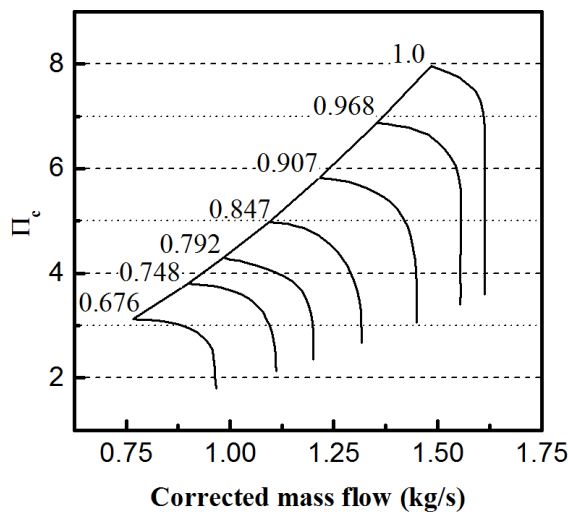
NOMENCLATURE		Greek symbols	
C	Specific heat capacity [J/(kg·K)]	λ	Evaporation constant [m ² /s]
D	Saut mean diameter [μm]	η	Efficiency [-]
d	Diameter of the bead thermocouple [m]	Π	Pressure ratio [-]
$F()$	Function	ρ	Density [kg/m ³]
f	Fuel air ratio [-]	μ	Viscosity [kg/(m·s)]
h	Heat transfer coefficient [W/(m ² ·K)]		
I	Mass momentum of inertia [kg·m ²]		
k	Ratio of specific heat capacity [-]		
kg	Conductivity [W/(m·K)]		
m	Mass flow rate [kg/s]		
N	Rotational speed [min ⁻¹]		
Nu	Nusselt number [-]		
P	Power [W]		
P_t	Total pressure [Pa]		
Pr	Prandtl number [-]		
Re	Reynolds number [-]		
S	Surface area of heat transfer [m ²]		
t	Time [s]		
T	Total temperature [K]		
Tq	Torque [Nm]		
U	Absolute velocity [m/s]		
V	Volume [m ³]		
		Subscripts	
		a	Air
		acc	Acceleration
		b	Combustor
		c	Compressor
		ce	Evaporation controlled combustion efficiency
		cor	Corrected value
		cr	Reaction controlled combustion efficiency
		g	Gas
		ref	Reference value
		std	Standard value
		$starter$	Engine starter
		t	Turbine
		tc	Thermocouple

The first step of the map extrapolation method is to rearrange the compressor map by introducing the corrected torque to avoid the discontinuity of efficiency in sub idle region. The most convenient way to derive corrected torque is to use the flow coefficient, corrected rotating speed and the efficiency, as these parameters are already well described in the conventional compressor maps. Using the Euler's equation in conjunction with the corrected

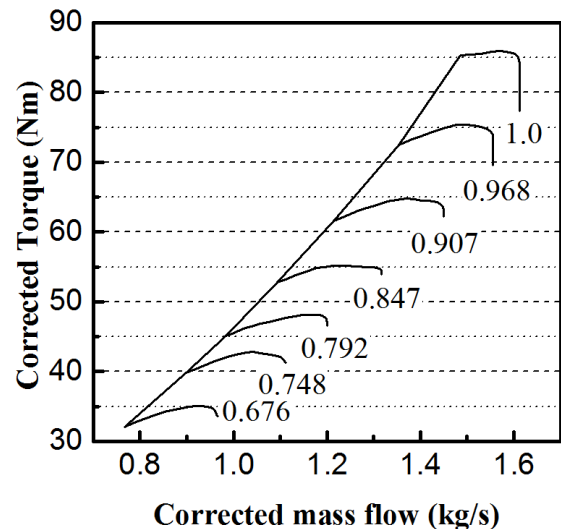
parameters of a turbo machinery, the quasi-dimensional torque group can be derived using Equation (1).

$$Tq_{cor} = \frac{30}{\pi} T_{std} C m_{cor} \left(\Pi_c^{(k-1)/k} - 1 \right) / (N_{cor} \eta_c) \quad (1)$$

The Allison 250 engine compressor map in terms of corrected mass flow, corrected torque and pressure ratio as functions of beta values and corrected rotating speed is shown in Figure 1.



(a) Pressure ratio



(b) Corrected torque

Figure 1. Compressor map rearrangement with corrected torque and pressure ratio

The second step is to generate the compressor zero speed line by conducting a locked rotor study. In Zachos' study, the single stage zero speed line was generated followed by the stage stacking method to get the zero speed line of the whole compressor. In this paper, the Allison 250 engine compressor zero speed line was deduced from the locked

rotor characteristic measurement data provided by Hönle [6].

With the zero speed line available, the beta lines are expanded by matching each point on the lowest above idle curve to the zero speed curve. And the final step of this method is to interpolate the speed lines between the zero speed curve and the lowest above idle curve. As is mentioned

by Zachos, the equations used for beta lines extrapolation and speed lines interpolation can be either linear or polynomial. In this study, a linear algorithm was used for both.

The complete extrapolated compressor map is shown in Figure 2.

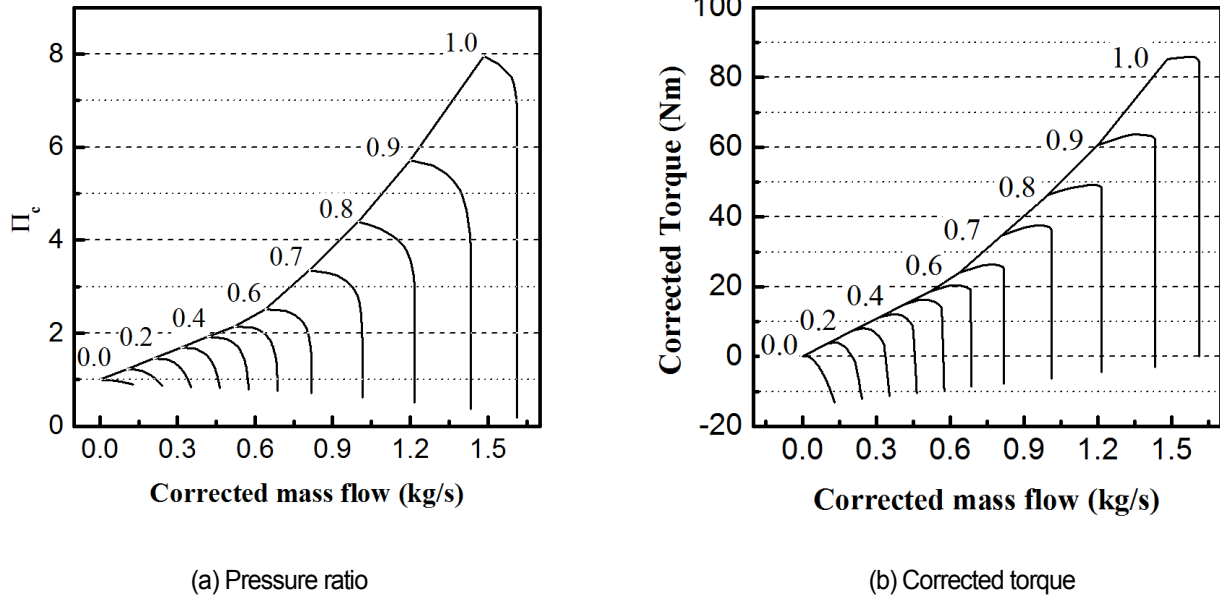


Figure 2. Compressor map extrapolation result

2. VALIDATION

The validation of the PECME method can be carried out by comparison between Allison engine starting performance simulation results and test data. During this section, some details regarding the validation method, such as the engine starting simulation model and the test data correction method, are initially discussed. Then the Allison engine starting performance simulation results using the extrapolated map are presented and validated with the test data.

2.1 Engine sub idle performance simulation

The so-called component map based engine performance simulation model in conjunction with the complete extrapolated compressor map is employed in this study to simulate the starting performance of the Allison engine. However some adjustments are required before this model can be used in sub idle region properly. Two main adjustments of the model, i.e. the power extrapolation model and the evaporation controlled combustion efficiency model, are discussed in this section.

2.1.1 Power extrapolation method

The component maps based engine simulation model should be used in the whole engine starting sequence for a complete validation of the extrapolated map. However, in starting simulation, it is found that the component maps based model encounters extremely poor convergence at the very beginning of the engine starting process, i.e. power turbine rotational speed close to zero. Thus, the so-called power extrapolation method was used at the very beginning of the engine starting process, to avoid model iteration

divergence.

The power extrapolation method was developed by Walsh and Fletcher [11] and was utilized by Gaudet [4] to build up the dynamic model of gas turbine engine starting sequence. This method is based on the assumption that the power of turbine machinery is proportional to the cube of its rotational speed.

$$\frac{P}{N^3} = \frac{P_{ref}}{N_{ref}^3} \quad (2)$$

Thus, the compressor power and the turbine power can be extrapolated along the speed line using Equation 2. With the starter power known, the acceleration power can be calculated by employing Equation 3. Furthermore, the spool acceleration/deceleration rate can also be deduced from the acceleration/deceleration power and the rotor's moment of inertia using Equation 4.

$$P_{acc} = P_{starter} + P_t - P_c \quad (3)$$

$$P_{acc} = \left(\frac{\pi}{30} \right)^2 \cdot I \cdot N \cdot \frac{dN}{dt} \quad (4)$$

2.1.2 Sub idle combustion efficiency

Engine combustion efficiency is mainly influenced by three factors: evaporation rates, mixing rates and reaction rates. However, the dominative factor varies according to the combustor working conditions. Although the combustion efficiency is rarely determined by three factors at the same time, it is inevitable that two or more factors participate in determining the overall efficiency where the combustor works in transition from one region to another [12].

A combustion efficiency model which is practical under a wide

range of working conditions was developed by Lefebvre [12]. In this model, the efficiencies controlled respectively by reaction, evaporation and mixing were calculated separately. The final combustion efficiency was obtained by multiplying the three efficiencies. Due to the fact that the mixing rates tend to be only limiting at conditions where the level of combustion efficiency is close to 100 percent, it is often preferable to express combustion efficiency as the product of the reaction efficiency and the evaporation efficiency [12]. The reaction controlled efficiency and the evaporation controlled efficiency are defined in Equation 5 and Equation 6 respectively.

$$\eta_{cr} = 1 - \exp \left[\frac{-0.002 P_{t_b}^{1.3} \cdot V_b \cdot \exp(T_b / 400)}{f_b \cdot \dot{m}_a} \right] \quad (5)$$

$$\eta_{ce} = 1 - \exp \left[\frac{-36 \cdot 10^6 P_{t_b} \cdot V_b \cdot \lambda}{T_b \cdot D^2 \cdot f_b \cdot \dot{m}_a} \right] \quad (6)$$

The Sauter mean diameter (D in Equation 6) of the Allison 250 engine was given by Sutton in reference [13]. The fuel evaporation coefficient (λ in Equation 6) is interpolated from the data provided by Lefebvre [12].

2.2 Test data correction

An Allison 250-C20B engine was installed on the engine test bed at the Institute for Flight Propulsion, in Technical University of Munich, see Figure 3. The test bed setup is introduced in detail in [14]. The measured parameters include the temperature and pressure at the ambient condition, the compressor outlet, the gas generator outlet and engine exhaust nozzle. Also the fuel mass flow rate, combustor outlet total pressure, rotational speeds and the torque on power turbine are measured.

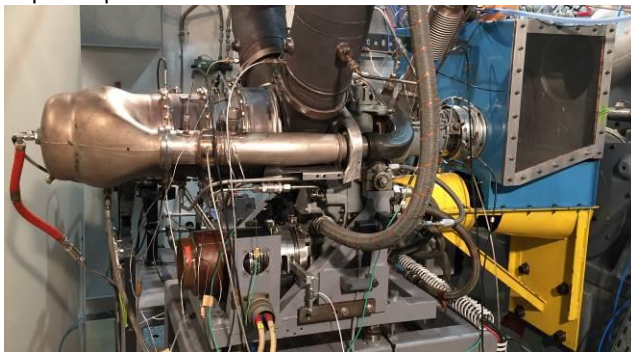


Figure 3. Allison 250 engine test bed in LFA, TUM.

Since the engine performance depends partially on the ambient conditions which usually differ according to the weather, the altitude and other conditions, it is necessary to correct the test data to standard conditions before they can be used to validate the simulation results. The correction equations can be found in [15] and [16].

Furthermore, the measured temperature is always time-delayed compared with the real data due to the thermo inertia effect of the thermocouple, which must be considered to ensure the comparability between simulation results and test data. A method to correct the temperature test data by calculating the thermo inertia effect was introduced by Liu [17]. In this method, the thermocouple is treated as a lump of material heated at uniform temperature, based on the

assumption that the diameter of the bead thermocouples is very small and the thermo conductivity of the thermocouple material is very high. Therefore, the lump heat capacity method was used to describe the heat balance of the thermocouple conjunction (Equation 7).

$$\bar{h}_{tc} S_{tc} (T_g - T_{tc}) = \rho_{tc} V_{tc} C_{tc} \frac{dT_{tc}}{dt} \quad (7)$$

The calculation of thermocouple heat transfer coefficient \bar{h}_{tc} is essential to obtain the corrected temperature from Equation 7. An empirical equation was provided in reference [18] to calculate the heat transfer coefficient:

$$Nu_d = \bar{h}_{tc} d / kg = F(Re_d, Pr) \quad (8)$$

In which $Re_d = \rho_g U_g d / \mu_g$ and $Pr = C_g \mu_g / kg$.

Additionally, Equation 7 can be not only used to correct the test data but also used to calculate the simulation results. In this study, Equation 7 was used in each time step during simulation to calculate the measured temperature which is actually the temperature of the thermocouple conjunction. A comparison between simulation results with and without considering the thermo inertia is shown in Figure 4. It is obvious that the simulation results considering the thermo inertia match the measured data much better.

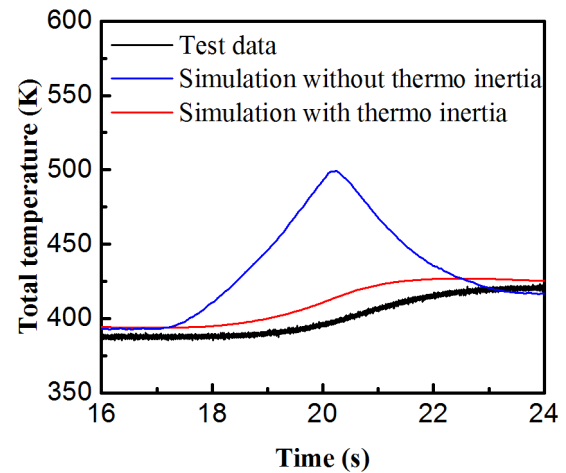


Figure 4. Influence of thermocouple inertia on measured data.

2.3 Validation

The Allison 250 turboshaft engine starting performance was simulated employing the extrapolated compressor map and the simulation model introduced above. The rotational speed simulation results of both gas generator and power turbine are shown in Figure 5 in comparison with test data. The deviations of gas generator rotational speed and power turbine rotational speed in some critical points are calculated and listed in Table 1 and Table 2 respectively.

As can be seen in Table 1, the maximum deviation of the gas generator rotational speed is around 23% at 30% the design speed. While the maximum deviation of the power turbine rotational speed, as is provided in Table 2, is around 22.7% at 15% the design speed. The maximum deviations are both detected during the period with the most dramatic acceleration, i.e. from 40s to 50s. Most of the relative

deviations of both the gas generator and the power turbine rotational speeds increase with the decreasing rotational speed. However, no such trend is found among the absolute deviations. The larger deviation at lower rotational speed is mainly caused by smaller denominators in relative deviation calculation.

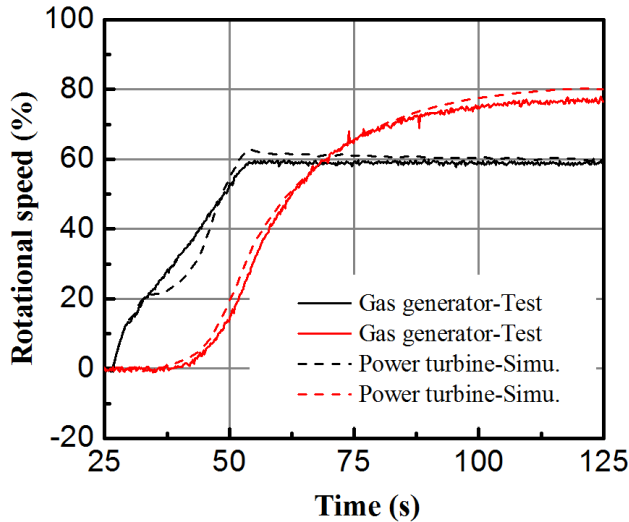


Figure 5. Rotational speed

Table 1. Deviations of gas generator rotational speed

Time [s]	Test	Simulation	Deviation	
			Absolute	Relative [%]
27	1.73	1.46	0.27	15.65
30	13.57	14.04	0.47	3.47
35	23.90	21.45	2.44	10.22
40	32.12	24.75	7.37	22.95
50	52.07	54.52	2.46	4.72
54	58.25	63.02	4.77	8.18
70	58.84	61.05	2.21	3.75
100	58.64	60.53	1.89	3.22
125	59.07	59.71	0.65	1.10

Table 2. Deviations of power turbine rotational speed

Time [s]	Test	Simulation	Deviation	
			Absolute	Relative [%]
40	1.67	1.96	0.29	14.88
45	5.38	6.49	1.11	17.07
50	14.84	19.20	4.36	22.72
54	28.23	32.81	4.58	13.95
70	61.13	60.67	0.46	0.76
100	74.76	77.47	2.71	3.50
125	77.35	80.14	2.79	3.49

The simulated gas generator operating line during the engine starting process is shown in Figure 6. The lowest gas generator operating speed is around 10% of the design

speed. For lower speed, the power extrapolation method is employed. Although the power extrapolation method was used at the beginning of the starting process, the operating line covers most of the sub idle speed lines. So the sub idle map validation is sufficient and valid.

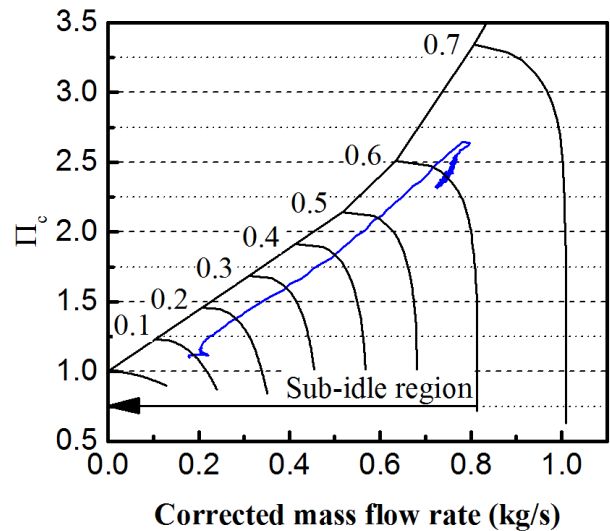


Figure 6. Gas generator operating line

3. CASE STUDY

In this section, the Allison 250 engine operating process from engine starting to 200Nm load is simulated and the simulation results are presented as a case study. The simulation results are again compared with test data to show the capability of the whole methodology introduced above. The operating process is described in Table 3.

Table 3. Engine test operating process

Phase	Time [s]	Operations
1	0-419	Standby
2	420-1089	Startup and steady running at idle rating
3	1090-1134	Power turbine torque step change to 50Nm and back
4	1135-1316	steady running at idle rating
5	1317-1618	Power turbine accelerating to 100% design speed and steady running
6	1619-2472	Accelerating to flight mode and steady running
7	2473-2646	Power turbine torque increases to 200Nm and steady running

As is shown in Figure 7, the rotational speeds simulation results match the test data well. The deviations at steady state are smaller than 5 percent, while the deviation of transient state is relatively larger. For instance, the deviation of phase 3 reaches 17 percent. This is due to the insufficient modelling of some transient effects such as the delay of the actuator in response to the commands of the engine controller. Figure 8

shows the total pressure at the power turbine in- and outlet. smaller than 5 percent, making for a good match. The deviations for both steady state and transient state are

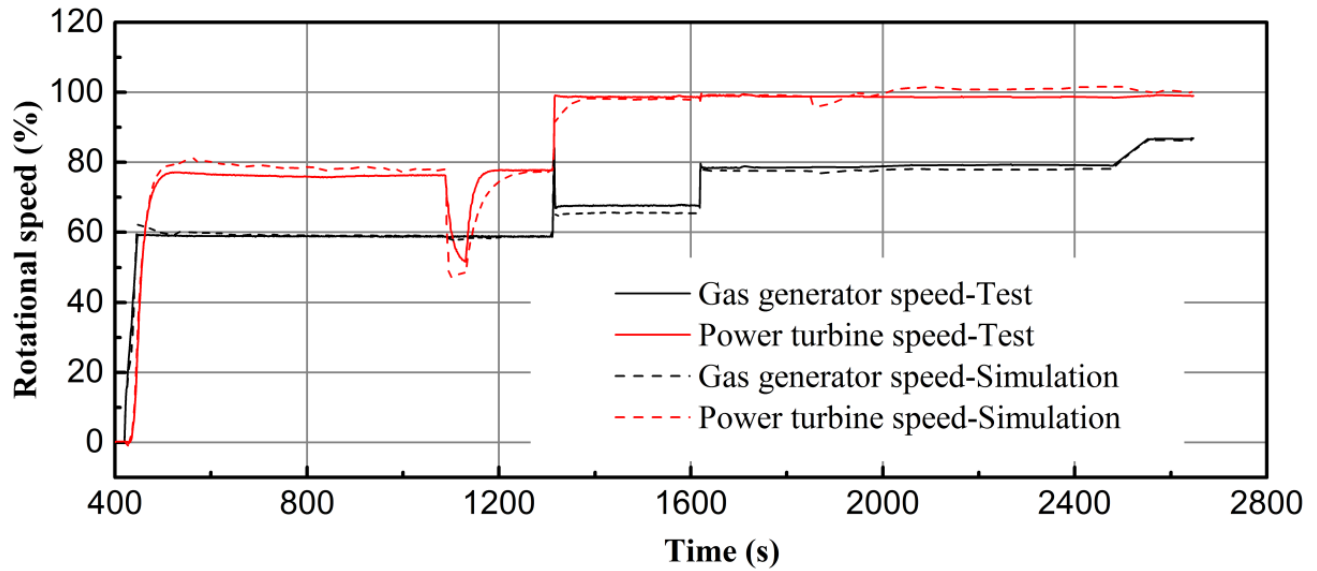


Figure 7. Rotational speed

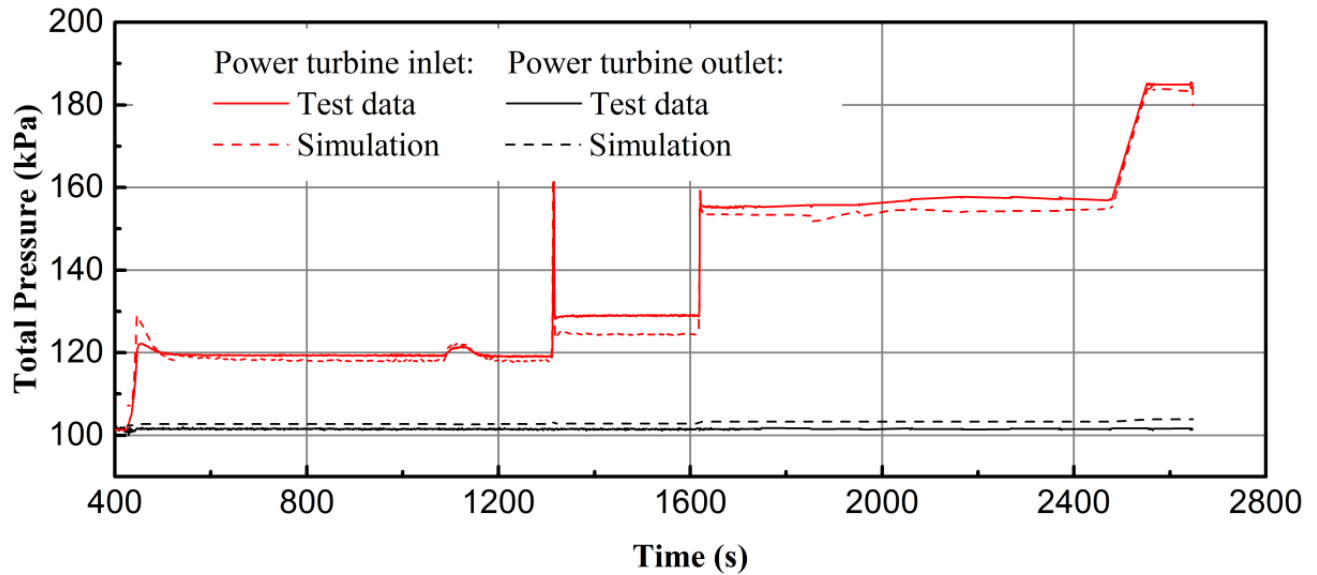


Figure 8. Total pressure at power turbine inlet and outlet

The temperature simulation results are all corrected using the method introduced in section 2.2 to match the test data. The total temperature at the compressor outlet and the gas generator outlet are shown respectively in Figure 9 and

Figure 10. The largest deviations of the temperature at these two stations are within 5 percent and 6 percent respectively, illuminating that the data correction method is practical and valid.

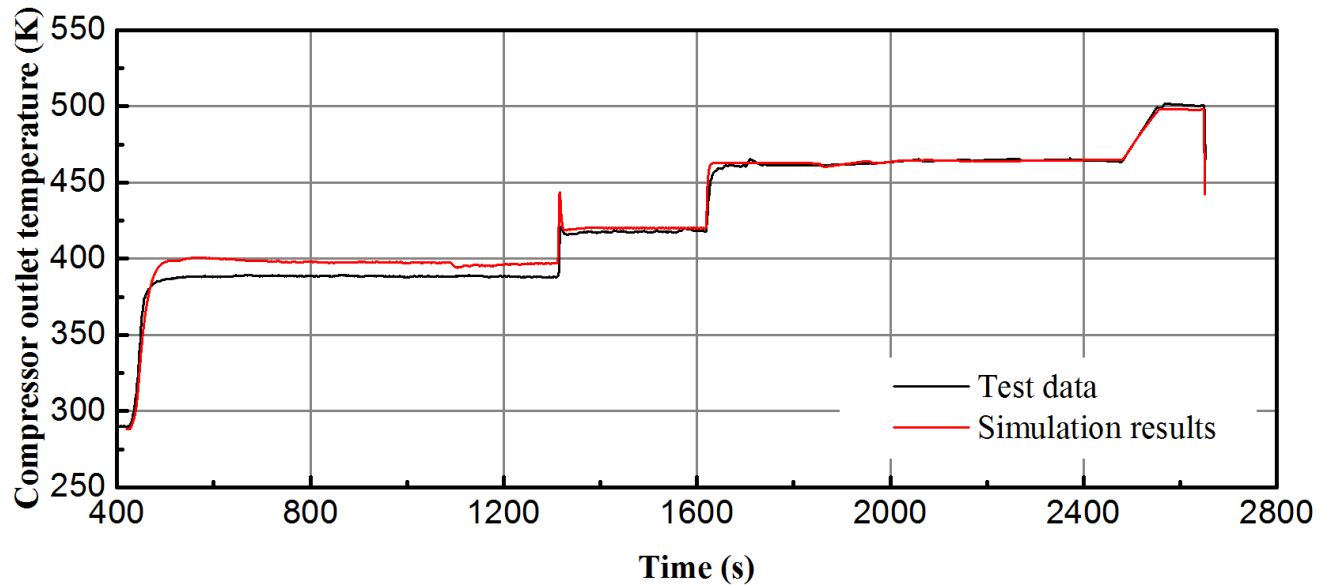


Figure 9. Total temperature at compressor outlet

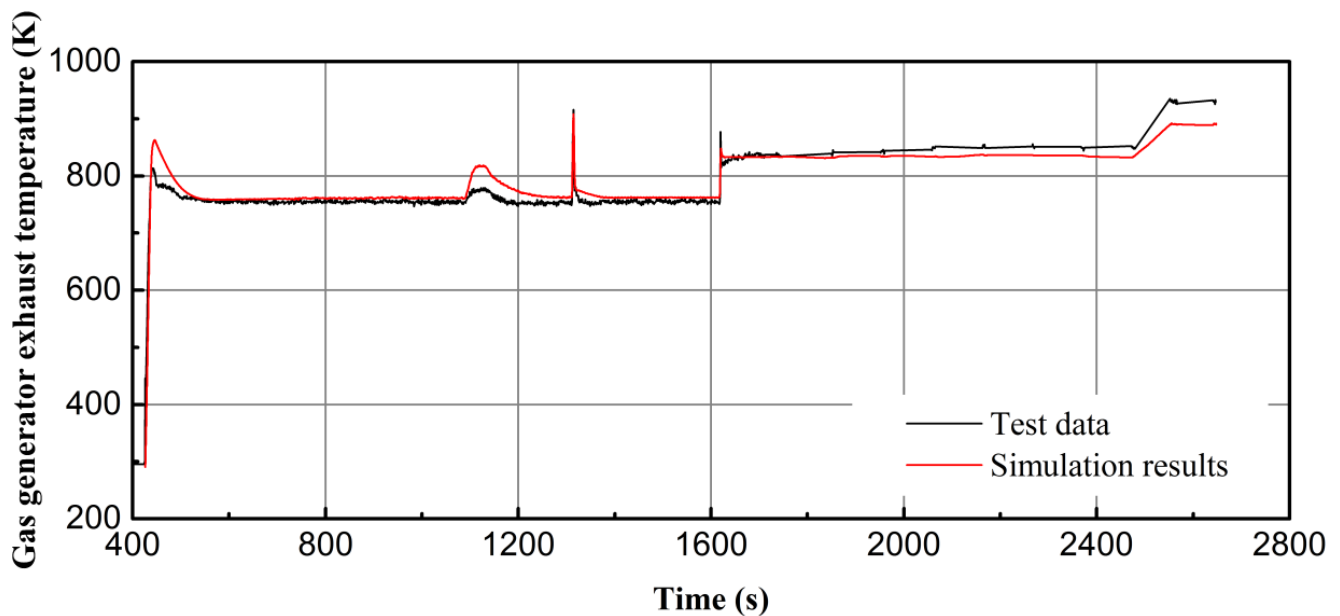


Figure 10. Gas generator exhaust temperature

4. CONCLUDING REMARKS

The Allison 250 engine compressor map was extrapolated employing the physically enhanced map extrapolation method. Then the complete compressor map was used in the engine starting performance simulation model to obtain the engine starting performance. The simulation results were validated with engine starting test data. The absolute deviations of the rotational speeds of both the gas generator and the power turbine are smaller than 7.5% and 5% of the design speeds respectively.

A case study of the Allison engine operating process from engine startup to 200Nm load is also provided and compared with the test data. The deviations of the total temperature at compressor outlet and the total pressure at power turbine in- and outlet are smaller than 5%. The deviation of the gas

generator exhaust temperature is within 6%.

The validation and case study illuminate that the methodology introduced in this paper is practical and can provide reasonable simulation results in a wide range of engine operation. The sub idle combustion model and test data correction method introduced in this paper can also be a guide for further gas turbine engine performance simulation.

ACKNOWLEDGMENTS

Hereby, the author would like to thank Dr. Wolfgang Erhard and Martin Kerler from the Institute for Flight Propulsion, Technical University of Munich for the test data they provided and their kind suggestions.

REFERENCES

- [1] Kurzke J. How to Get Component Maps for Aircraft Gas Turbine Performance Calculations. International Gas Turbine and Aeroengine Congress and Exhibition. Birmingham, UK, 1996: 7.
- [2] Riegler C, Bauer M, Kurzke J. Some aspects of modeling compressor behavior in gas turbine performance calculations. ASME Turbo Expo 2000, Munich Germany, 2000-GT-574.
- [3] Sexton W. R. A method to control turbofan engine starting by varying compressor surge valve bleed. Master. Blacksburg Virginia: Virginia Polytechnic Institute and State University, 2001.
- [4] Gaudet S R. Development of a Dynamic Modeling and Control System Design Methodology for Gas Turbines [D]. Ottawa, Ontario, Canada : Carleton University , 2007.
- [5] Gaudet S.R., Gauthier J.D. A simple sub-idle component map extrapolation method. ASME Turbo Expo 2007: Power for Land, Sea, and Air. 2007: 29-37.
- [6] Hönle J, Kerler M, Nachtigall H, Erhard W, Kau H-P. Experimental validation of a sub-idle compressor map extrapolation. 21st ISABE conference. Busan, Korean, 2013: 7.
- [7] Jones G, Pilidis P, Curnock B. Extrapolation of compressor characteristics to the low-speed region for sub-idle performance modelling. ASME Turbo Expo 2002, 2002: 861-67.
- [8] Howard J. Sub-idle modelling of gas turbines: Altitude relight and windmilling. Cranfield: Cranfield University, 2007.
- [9] Zachos P. K. Gas turbine sub-idle performance modelling: altitude relight and windmilling. Cranfield : Cranfield University, 2010.
- [10] Aslanidou I, Zachos P. K, Pachidis V, Singh R. A physically enhanced method for sub-idle compressor map generation and representation. ASME Turbo Expo 2010, Glasgow, Scotland, UK, GT2010-23562.
- [11] Walsh P P, Fletcher P. Gas Turbine Performance [M]. , Blackwell Science, Oxford, 2004.
- [12] Lefebvre A H. Fuel effects on gas turbine combustion[R]. Wright-Patterson AFB, oh 45433: Aero Propulsion Laboratory, 1983.
- [13] Sutton R D, Troth D L, Miles G A. Analytical Fuel Property Effects-Small Combustors[R]. Indianapolis, Indiana: Alison Gas Turbine Division, General Motors Corporation, 1984.
- [14] M. Kerler, J. Hönle, W. Erhard, H.-P. Kau: "Helicopter Engine-in-the-Loop Test Setup", 39th European Rotorcraft Forum, Moscow, Russia, September 3rd-6th, 2013
- [15] Kurzke J. Model based gas turbine parameter corrections[C]. American Society of Mechanical Engineers, 2003.
- [16] Xiaochun L, Hu W. Aero Engine Principles, Chapter 7 [M]. Northwestern Polytechnical University Press, Xi'an, 2005.
- [17] Liu C, Von Wolfersdorf J, Zhai Y. Time-resolved heat transfer characteristics for steady turbulent flow with step changing and periodically pulsating flow temperatures[J]. International Journal of Heat and Mass Transfer, 2014, 76: 184-198.
- [18] Bejan A, Kraus A D. Heat transfer handbook[M]. 1 ed. John Wiley & Sons, 2003.